Available online at www.sciencedirect.com
ScienceDirect
Journal of Magnetic Resonance 182 (2006) 29–37
JMR Journal of Magnetic Resonance
www.elsevier.com/locate/jmr

Selective *J*-resolved spectra: A double pulsed field gradient spin-echo approach

Federico Rastrelli *, Alessandro Bagno

Dipartimento di Scienze Chimiche, Università di Padova, via Marzolo 1, 35131 Padova, Italy

Received 15 March 2006; revised 24 April 2006
Available online 27 June 2006

Abstract

A simple method to obtain selective *J*-resolved spectra is presented, which relies on the refocusing properties of double pulsed field gradient spin-echoes and provides unambiguous assignment of the measured coupling constants. The proposed examples show how this method is of general applicability, and requires no more than a simple optimization strategy to produce artifact-free spectra. Examples of application include the determination of a small, long-range coupling constant (0.7 Hz) in *trans*-retinal and H^{α} couplings in a tripeptide.
© 2006 Elsevier Inc. All rights reserved.

Keywords: PFGSE; *J*-resolved; Selective refocusing; Double spin-echo

1. Introduction

In the varied family of 2D NMR correlation techniques, *J*-resolved spectroscopy occupies a distinguished role in that it can separate the joint effects of chemical shifts and scalar couplings (either homo- or hetero-nuclear) by storing them into different spectral dimensions. In the homonuclear version, a *J*-resolved experiment produces a spectrum $S(\omega_1, \omega_2)$ where the hyperfine structure relative to each chemical shifted signal is tilted by 45° in the (ω_1, ω_2) plane. Additional post-processing (that is, a shear of factor 1) then realizes the transformation $S(\omega_1, \omega_2) \rightarrow S(J, \delta)$, such that a projection onto the δ dimension yields a fully homodecoupled spectrum also known as "chemical shift spectrum" [1]. On the other hand, cross-sections taken along each of the chemical shift signals will reproduce just the associated hyperfine patterns from which coupling constants can be conveniently extracted.

However, even when a target shift and its relative hyperfine pattern have been clearly isolated, conventional *J*-resolved spectroscopy does not *per se* allow for unambiguous assignment of the measured coupling constants, which somehow limits the applicability of the approach (see Fig. 1).

Despite this shortcoming, *J*-resolved techniques are advantageous in that the chemical shift or *J*-coupling information is presented in a way that easily lends itself to quantitative determination. For this reason they are regaining popularity since quantum-chemistry methods have become capable of predicting NMR parameters [2], and it is obviously desirable to have a reliable database for validation [3,4].

To overcome this stumbling block one might resort to selective *J*-resolved experiments such as SERF [5], which can reveal mutual couplings between single spin pairs. Nonetheless, the SERF method heavily relies on selective pulses in both the excitation of the target resonance and in the selective refocusing of the coupled partner, therefore making its practical implementation sensitive to the odd phase behaviour typical of selective pulses.

By exploiting a combination of excitation sculpting [6] and double-quantum filtration, Bourg and Nuzillard have proposed a biselective *J*-resolved pulse sequence that delivers the same information as SERF with a more robust approach [7]. Following a similar strategy, in this paper we devise an alternate, simple NMR experiment to obtain

* Corresponding author. Fax: +39 0498275239.
E-mail address: federico.rastrelli@unipd.it (F. Rastrelli).

1090-7807/$ - see front matter © 2006 Elsevier Inc. All rights reserved.
doi:10.1016/j.jmr.2006.06.004

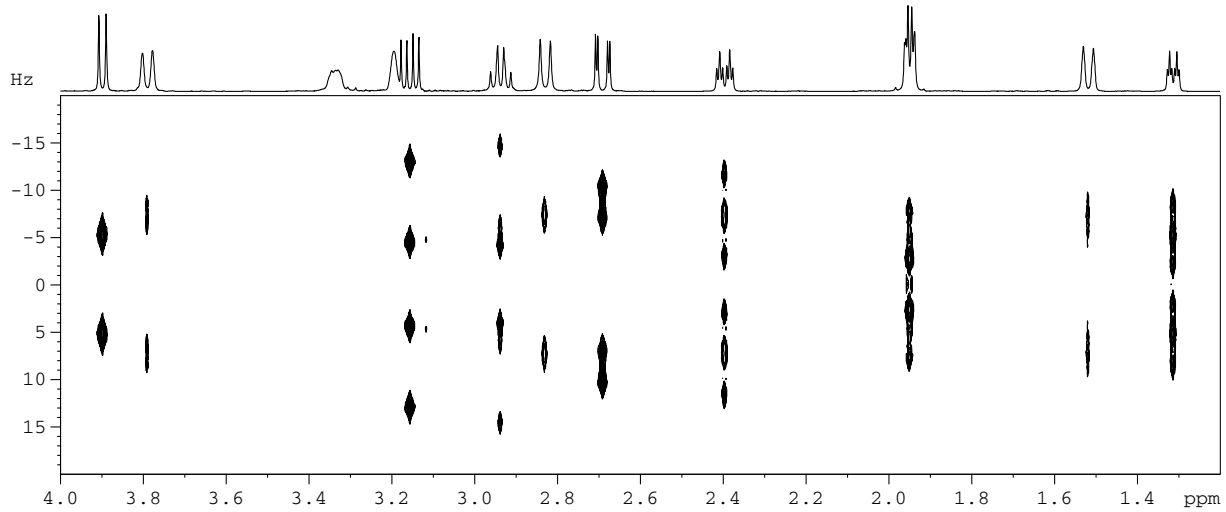

Fig. 1. In a standard *J*-resolved spectrum (e.g., from a strychnine sample, above), all the couplings are active and evolve simultaneously in the indirect dimension. As such, sorting out the value of *J* for a specific spin pair requires a collateral knowledge, which is then discarded, on the entire coupling network relative to the same spins. Overcoming this "all-or-nothing" issue is often time consuming even when the spectral assignments are well established, and high-field instruments are of little help in the simplification of this task. Moreover, the spectral window in the *J*-dimension is actually limited by the widest multiplet pattern, which lowers the resolution necessary to measure small *J*-couplings. The spectrum was recorded at 600 MHz with a standard *J*-resolved pulse sequence. Eight scans were collected for each of the 64 t_1 increments. The standard processing (apodization with unshifted sinebell functions in both dimensions and magnitude mode display) was complemented with symmetrization. Top trace shows a full ^{1}H spectrum.

(bi)selective *J*-resolved spectra. It will be shown that this method is of general applicability and requires in principle nothing more than a simple optimization of soft refocusing pulses.

2. Theory

Some transformation properties of pulsed field gradient spin-echoes (PFGSEs) are justified in this section by means of the density operator approach. In doing so, we will be finally interested in deriving the matrix **T** which defines the linear transformation

$$\mathbf{M} = \mathbf{T} \cdot \mathbf{m}(0) \tag{1}$$

carried out by a PFGSE propagator, given an input magnetization vector $\mathbf{m}(0)$ whose relevant components are specified for each case.

It is customary for the density operator describing a system of N spins $I_1, I_2, \ldots, I_N$ to be expanded on a set of basis operators B_s as [8]

$$\sigma(t) = \sum_s b_s(t) B_s. \tag{2}$$

In dealing with spins 1/2, the complete basis set $\{B_s\}$ consists of 4^N product operators of the form

$$B_s = B_s^{(1)} \otimes B_s^{(2)} \otimes \cdots \otimes B_s^{(N)}, \quad B_s^{(k)} \in \{E_k, I_{kx}, I_{ky}, I_{kz}\} \tag{3}$$

and it follows from the orthogonality property $\mathrm{Tr}\{B_r B_s\} = \delta_{rs} 2^{N-2}$ that at each timepoint t the (normalized) magnetization components in the physical space can be calculated from the trace relation

$$M_\alpha(t) = \mathrm{Tr}\{I_\alpha \sigma(t)\}, \tag{4}$$

where $I_\alpha = \sum_k I_{k\alpha}$ for $\alpha = x$, y or z.

In the following treatment, pulsed field gradient spin-echoes are introduced which consist of whatever refocusing element S enclosed by two equal field gradient pulses to form the cluster $[G - S - G]$. For our purposes it will prove convenient to write the refocusing element as a composite rotation operator acting on spin k

$$S_k = \mathrm{e}^{-\mathrm{i}\beta_k I_{kz}} \mathrm{e}^{-\mathrm{i}\theta_k I_{ky}} \mathrm{e}^{-\mathrm{i}\alpha_k I_{kx}} \mathrm{e}^{+\mathrm{i}\theta_k I_{ky}} \mathrm{e}^{+\mathrm{i}\beta_k I_{kz}}, \tag{5}$$

where α is the flip angle, θ is the tilt angle (defined such that $\theta = \pi/2$ on-resonance) and β is the phase. In this way, the magnetization components transformed upon application of a $[G - S_k - G]$ cluster can be expressed through Eq. (4) as

$$M_{k\alpha} = \frac{1}{2\pi} \int_0^{2\pi} \mathrm{d}\phi \, \mathrm{Tr}\left\{ I_{k\alpha} \mathrm{e}^{-\mathrm{i}\phi I_z} S_k \mathrm{e}^{-\mathrm{i}\phi I_z} \sigma(0) \mathrm{e}^{\mathrm{i}\phi I_z} S_k^\dagger \mathrm{e}^{\mathrm{i}\phi I_z} \right\}, \tag{6}$$

being ϕ the spatially dependent phase induced by the magnetic field gradients and $\sigma(0)$ the density operator at some chosen zero-time.

2.1. Biselective PFGSE

The case of a PFGSE that incorporates a generic refocusing element S has been elucidated by Hwang and Shaka [6]: following the same approach, we now want to consider the case of a PFGSE that includes a biselective refocusing element $S = S_1 S_2$. For future convenience, we will extend our treatment to also include antiphase magnetization and longitudinal two-spin order, that is, we will complement the zero-time density operator with the product operator subset $\{2I_{kx}I_{lz}, 2I_{ky}I_{lz}, 2I_{1z}I_{2z}\}$ with $k, l = 1, 2$ and $k \neq l$.

Given the symmetry properties of the problem, we can consider only the density operator relative to spin 1. Thus, beginning with

$$\sigma_1(0) = m_{1x}I_{1x} + m_{1y}I_{1y} + m_{1z}I_{1z} + m_{1xz}2I_{1x}I_{2z} + m_{1yz}2I_{1y}I_{2z} + m_{zz}2I_{1z}I_{2z}, \tag{7}$$

the overall transformation matrix is found to be block-diagonal

$$\mathbf{T}_1 = \begin{pmatrix} \mathbf{T}_1' & 0 \\ 0 & \mathbf{T}_1'' \end{pmatrix}, \tag{8}$$

where the block relative to in-phase (m_{1x}, m_{1y}) and longitudinal (m_{1z}) magnetization is

$$\mathbf{T}_1' = \begin{pmatrix} P_1\cos 2\beta_1 & P_1\sin 2\beta_1 & 0 \\ P_1\sin 2\beta_1 & -P_1\cos 2\beta_1 & 0 \\ 0 & 0 & 1-2P_1 \end{pmatrix} \tag{9}$$

and the block relative to anti-phase magnetization (m_{1xz}, m_{1yz}) and longitudinal two-spin order (m_{zz}) is

$$\mathbf{T}_1'' = (1-2P_2)\mathbf{T}_1', \tag{10}$$

$P_k = 1/2(1 - M_{kz}/m_{kz})$ being the probability that spin k is flipped by S_k. Upon exchange of the indexes 1 and 2, the above results hold for spin 2 and we see that a double PFGSE removes any phase defects which depend on β_1, since

$$\mathbf{T}_1 \cdot \mathbf{T}_1 = \begin{pmatrix} (\mathbf{T}_1')^2 & 0 \\ 0 & (\mathbf{T}_1'')^2 \end{pmatrix}, \quad \text{with} \quad (\mathbf{T}_1')^2 = \begin{pmatrix} P_1^2 & 0 & 0 \\ 0 & P_1^2 & 0 \\ 0 & 0 & (1-2P_1)^2 \end{pmatrix}. \tag{11}$$

An extension of the above results also suggests how a train of selective pulses can achieve clean multi-selective refocusing, which has been shown by Parella *et al.* in Ref. [9].

2.2. Modulated biselective PFGSE

A modulated biselective PFGSE consists of the cluster $t - [G - S_1S_2 - G] - t$: in order to treat this case, Eq. (6) must be modified as follows:

$$M_{k\alpha}(t) = \frac{1}{2\pi}\int_0^{2\pi} \mathrm{d}\phi\, \mathrm{Tr}\{I_{k\alpha}\, \mathrm{e}^{-\mathrm{i}Ht}\, \mathrm{e}^{-\mathrm{i}\phi I_z} S\, \mathrm{e}^{-\mathrm{i}\phi I_z}\, \mathrm{e}^{-\mathrm{i}Ht} \sigma(0)\, \mathrm{e}^{\mathrm{i}Ht} \times \mathrm{e}^{\mathrm{i}\phi I_z} S^\dagger\, \mathrm{e}^{\mathrm{i}\phi I_z}\, \mathrm{e}^{\mathrm{i}Ht}\}, \tag{12}$$

where H is the unperturbed weak coupling Hamiltonian

$$H = \sum_k \omega_k I_{kz} + \sum_{k<l} \pi J_{kl}(2I_{kz}I_{lz}). \tag{13}$$

If the effects of the nested operators in Eq. (12) are regarded as cascaded transformations, it can be seen that the propagator $t - [G - S_1S_2 - G] - t$ as a whole will span rotations within the operator subspaces

$$\{I_{1x}, I_{1y}, I_{1z}, 2I_{1x}I_{2z}, 2I_{1y}I_{2z}, 2I_{1z}I_{2z}\}, \quad \{I_{2x}, I_{2y}, I_{2z}, 2I_{1z}I_{2x}, 2I_{1z}I_{2y}, 2I_{1z}I_{2z}\}, \tag{14}$$

so that, again, we can restrict our investigation to spin 1. Thus, when we expand the magnetization vector as

$$\mathbf{m}_1 = (m_{1x}, m_{1y}, m_{1z}, m_{1xz}, m_{1yz}, m_{zz}) \tag{15}$$

and we make use of Eqs. (12) and (13), we obtain the following transformation matrix for the modulated biselective PFGSE:

$$\mathbf{L}_1(t) = \begin{pmatrix} k_2^+(t)P_1\cos 2\beta_1 & k_2^+(t)P_1\sin 2\beta_1 & 0 & l_2(t)P_1\sin 2\beta_1 & -l_2(t)P_1\cos 2\beta_1 & 0 \\ k_2^+(t)P_1\sin 2\beta_1 & -k_2^+(t)P_1\cos 2\beta_1 & 0 & -l_2(t)P_1\cos 2\beta_1 & -l_2(t)P_1\sin 2\beta_1 & 0 \\ 0 & 0 & 1-2P_1 & 0 & 0 & 0 \\ -l_2(t)P_1\sin 2\beta_1 & l_2(t)P_1\cos 2\beta_1 & 0 & k_2^-(t)P_1\cos 2\beta_1 & k_2^-(t)P_1\sin 2\beta_1 & 0 \\ l_2(t)P_1\cos 2\beta_1 & l_2(t)P_1\sin 2\beta_1 & 0 & k_2^-(t)P_1\sin 2\beta_1 & -k_2^-(t)P_1\cos 2\beta_1 & 0 \\ 0 & 0 & 0 & 0 & 0 & (1-2P_1)(1-2P_2) \end{pmatrix}, \tag{16}$$

where the echo modulation is accounted for by the time-dependent quantities

$$k_2^+(t) = 1 - P_2 + P_2\cos(2\pi J_{12}t), \tag{17a}$$

$$k_2^-(t) = 1 - P_2 - P_2\cos(2\pi J_{12}t), \tag{17b}$$

$$l_2(t) = P_2\sin(2\pi J_{12}t). \tag{17c}$$

Still there is a dependence of $\mathbf{L}_1(t)$ on the phase β_1, arising from the refocusing element S_1; moreover, $\mathbf{L}_1(t)$ is not block-diagonal as in the case of a biselective PFGSE due to the inclusion of free evolution periods (note that, for $t = 0$, such blocks vanish and the overall matrix correctly reduces to $\mathbf{T}_1$).

In order to further remove the β_1 dependence resulting after a modulated biselective PFGSE sequence we are thus left with two basic choices, the first of which is to append a non-modulated biselective PFGSE and obtain the overall transformation

$$\mathbf{M}_1(t) = \mathbf{L}_1(0) \cdot \mathbf{L}_1(t) \cdot \mathbf{m}_1. \tag{18}$$

To evaluate Eq. (18), let us start with the density operator obtained right after the application of a hard RF pulse on a two-spin system in thermodynamic equilibrium [8]. Then, in the high-temperature approximation we may write for spin 1

$$\sigma_1(0) = m_{1x}I_{1x} + m_{1y}I_{1y} + m_{1z}I_{1z} \tag{19}$$

so that the explicit form of Eq. (18) becomes

$$\begin{pmatrix} M_{1x}(t) \\ M_{1y}(t) \\ M_{1z}(t) \\ M_{1xz}(t) \\ M_{1yz}(t) \\ M_{zz}(t) \end{pmatrix} = \begin{pmatrix} P_1^2[1 - P_2 + P_2\cos(2\pi J_{12}t)]m_{1x} \\ P_1^2[1 - P_2 + P_2\cos(2\pi J_{12}t)]m_{1y} \\ (1 - 2P_1)^2 m_{1z} \\ P_1^2P_2[1 - 2P_2]\sin(2\pi J_{12}t)m_{1y} \\ -P_1^2P_2[1 - 2P_2]\sin(2\pi J_{12}t)m_{1x} \\ 0 \end{pmatrix}. \tag{20}$$

Setting $t = t_1/2$, Eq. (18) translates experimentally into the pulse scheme of Fig. 2a. Building on the same arguments, a second possibility to remove the β_1 dependence is to replicate the modulated biselective PFGSE and obtain the overall transformation

$$\mathbf{M}_1(t) = \mathbf{L}_1(t) \cdot \mathbf{L}_1(t) \cdot \mathbf{m}_1. \tag{21}$$

This case is implemented by the double spin-echo pulse scheme of Fig. 2b (being $t = t_1/4$) and leads, in the limit of $P_1 = P_2 = 1$, to the same evolution rules found in Eq. (20).

In summary, both strategies lead to a biselective *J*-resolved spectrum where the signals of spins 1 and 2 evolve under their mutual scalar coupling J_{12} in the indirect dimension while the passive couplings appear in the direct dimension.

Clearly, the above treatment assumes the soft pulses to be short with respect to $1/J_{12}$, what is indeed an unrealistic approximation. Particularly when high selectivity is required, *J*-evolution throughout the duration of the soft pulses (typically tens of milliseconds) may add antiphase contributions to the observed signals. Yet, since these contributions are constant, they do not interfere with the echo modulation and are removed by the magnitude post-processing. In this same context, one may ask whether a second $G - S_1S_2 - G$ cluster is really necessary to remove the phase defects introduced by the first pair of refocusing pulses, since all of the phase errors will simply disappear in the magnitude processing. While this is certainly so for a standard FT-based spectral analysis, more refined processing protocols exist that require better control on the signal phase and that may benefit from the proposed approach [10,11]. Insertion of a second pair of refocusing pulses also delivers another advantage stemming from the enhanced selectivity of DPFGSE with respect to its PFGSE counterpart. This is particularly important in crowded spin systems, where an accidental refocusing of resonances other than the target ones may "activate" unwanted passive couplings.

Also, an implicit assumption has been made that the gradient pairs are uncorrelated so to avoid any accidental refocusing. While this is easily achieved in the experimental practice if the gradient pairs are applied along orthogonal axes, the situation is not trivial in the more typical case where all PFGs need to be applied along the same axis. In this context, the reader is referred to Ref. [12] for a thorough discussion on proper experimental settings.

3. Experimental

The pulse sequences outlined in the previous section have been put to test on samples of aspirin (**1**, Fig. 3) and strychnine (**2**) dissolved in $CDCl_3$, as well as all *trans*-retinal (**3**) dissolved in CD_2Cl_2; a 10 mM sample of the tripeptide f-Met-Leu-Phe-OMe (**4**) dissolved in CD_3CN was also investigated.

Measurements relative to compounds **1** and **4** were carried out on a Bruker Avance DRX 300 spectrometer equipped with a 5-mm BBO *z*-gradient inverse probe, while measurements relative to compounds **2** and **3** were carried out on a Bruker Avance DMX 600 spectrometer equipped

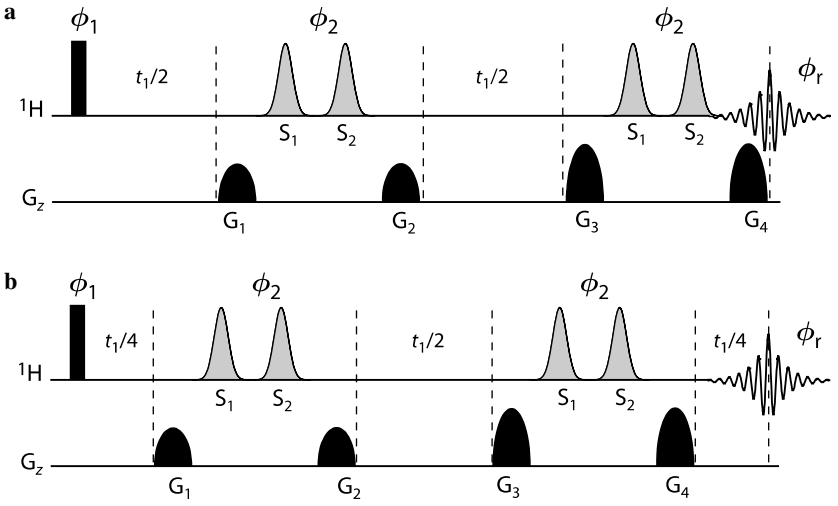

Fig. 2. Pulse sequences for biselective *J*-resolved experiments. (a) Single spin-echo; (b) double spin-echo. Black rectangles represent a π/2 hard pulse; soft π pulses S_1 and S_2 (in gray) are generically represented as Gaussian envelopes. Phase cycle: $\phi_1 = x, -x, x, -x$; $\phi_2 = x, y, -x, -y$; $\phi_r = -x, x, -x, x$. Gradient pairs are set to $G_1 = G_2$ and $G_3 = G_4$, and all gradient pulses are followed by a 100 μs recovery delay (not shown).

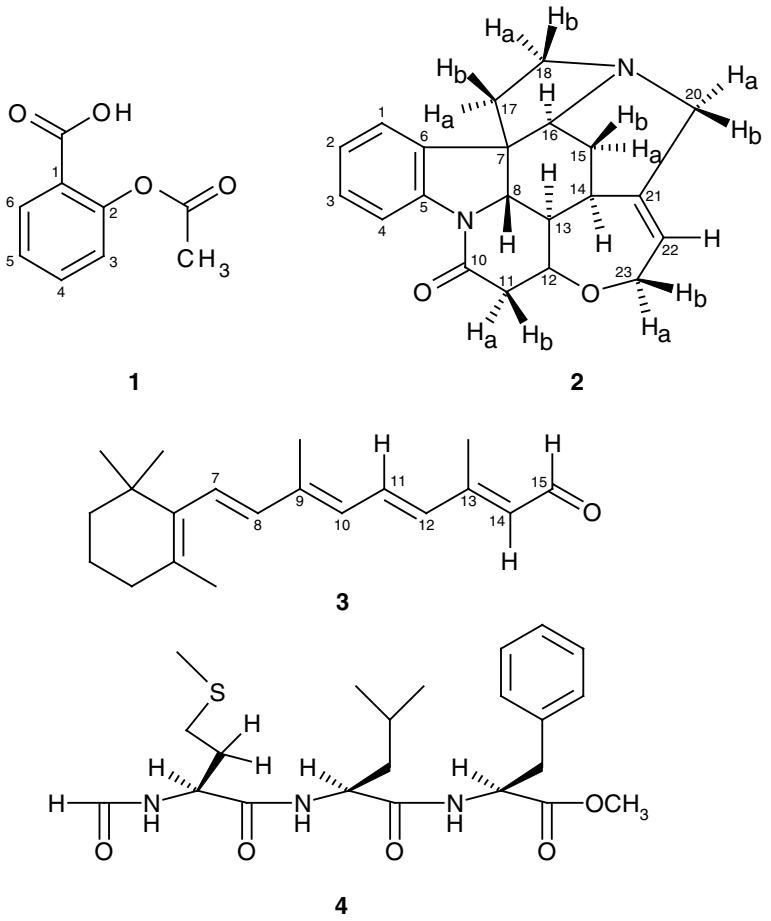

Fig. 3. Structure of 2-acetoxybenzoic acid (aspirin) (**1**), strychnine (**2**), all *trans*-retinal (**3**) and the tripeptide f-Met-Leu-Phe-OMe (**4**) with conventional labeling.

with a 5-mm TXI *xyz*-gradient inverse probe. Since the employed soft pulses need not necessarily belong to the same family, various combinations of different shapes for S_1 and S_2 have been tested: unless otherwise stated, the selective pulses S_1 and S_2 were Gaussian-shaped of 5% truncation level and about 20 ms duration. The duration of all gradient pulses (sine-shaped) was 600 μs and the set intensities were ca. 11 and 21 G/cm for the first and second pair, respectively.

All the *J*-resolved spectra presented hereafter have been processed using unshifted sinebell functions in both dimensions prior to Fourier transformation, and are displayed in magnitude mode (alternate protocols including symmetrization are indicated in the figure captions). Being the simplest approach to cope with the detrimental phase-twist lineshape, the use of strong weighting functions in "pseudo-echo" apodization is well known to introduce severe sensitivity losses and distortion of intensities [13]. A detailed analysis of these effects is beyond the scope of this work: in our case, we just observe that shifting the phase of the sinebell window in the indirect dimension did not affect the position of the resulting maxima at the observed digital resolution. Indeed, as pointed out before, sophisticated processing methods have been developed that attack the phase-twist problem on different grounds [10,11], but these are not yet established as a standard practice.

3.1. Soft pulses optimization

Before running any *J*-resolved experiments, optimization of the soft pulses S_1 and S_2 is recommended in order to maximize the aforementioned probabilities P_1, P_2 and avoid the breakthrough of annoying spectral artifacts (see next paragraph). To this aim, the power of the soft pulses S_1 and S_2 was independently varied within an array of bisselective DPFGSE experiments, until a maximum of signal intensity was observed from each of the refocused spectral bands.

4. Results and discussion

4.1. Suppression of spectral artifacts

When the probabilities P_1, P_2 deviate from unitary values, some extra peaks may appear in the *J*-dimension due to residual non-refocused magnetization. Even though the exact position and intensity of such peaks in the $S(J,\delta)$ spectrum can be calculated only by solving the full

density matrix problem, some information on the occurrence of artifacts in the indirect dimension is provided by inspection of explicit transformation rules like those of Eq. (20). As such, in the case of a single spin-echo sequence, J-modulation of in-phase magnetization in the indirect dimension occurs on spin 1 as

$$k_2^+(t) = (1 - P_2) + P_2 \cos(\pi J_{12} t_1) \tag{22}$$

so that an imperfect refocusing by S_2 (that is, $P_2 < 1$) would cause an extra peak at $\omega_1 = 0$ to appear in the corresponding J-projection. Similarly, in the case of the double spin echo, J-modulation in the indirect dimension occurs as

$$k_2^+(t)^2 - l(t)^2 = (1 - P_2)^2 + 2P_2(1 - P_2)\cos\left(\frac{1}{2}\pi J_{12} t_1\right) + P_2^2 \cos(\pi J_{12} t_1) \tag{23}$$

whence an imperfect refocusing by S_2 would cause extra peaks to appear at $\omega_1 = 0$ and $\omega_1 = \pm\pi J_{12}/2$. A full simulation of the artifactual patterns arising from imperfect refocusing is presented in Fig. 4 for single and double spin-echo pulse sequences.

In both cases, the artifacts at $\omega_1 \neq 0$ can be eliminated by symmetrization of the resulting $S(J, \delta)$ spectra, and the choice between the two pulse schemes is rather dictated by the $\omega_1 = 0$ artifacts being smaller in the case of the double spin-echo.

Besides the aforementioned advantages, the combined use of double spin-echoes and symmetrization post-processing has been recently proposed as a simple method to eliminate the so-called "strong coupling artifacts" [14]. In our context it is important to note that these unwanted signals usually span a larger frequency range than expected on

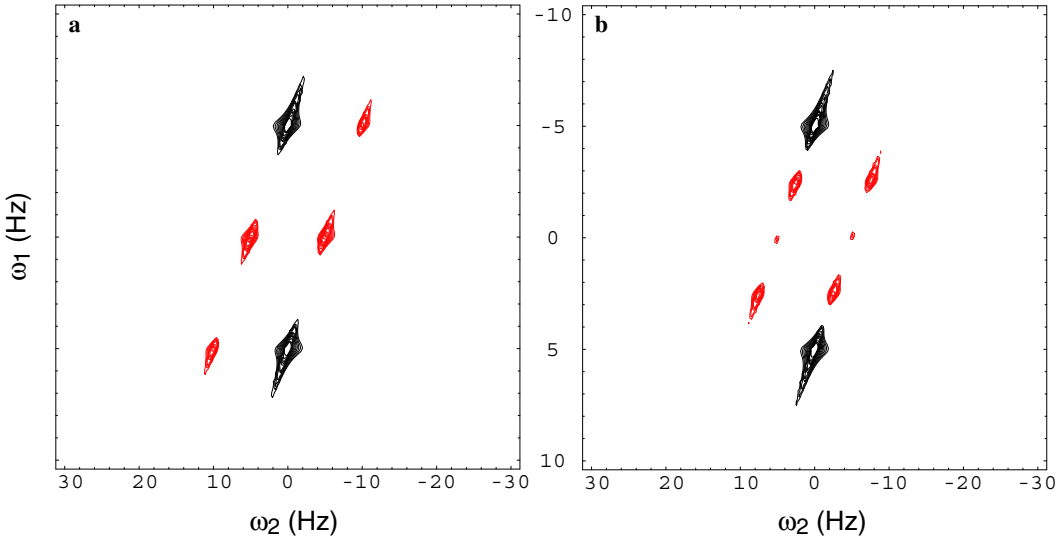

Fig. 4. Artifactual patterns (in red) calculated for spin 1, as resulting from imperfect refocusing of spin 2. The $S(J, \delta)$ spectra refer to (a) single spin-echo; (b) double spin-echo pulse scheme. The adopted parameters are: $P_1 = 1.0$, $P_2 = 0.7$, $T_2 = 3$ s, $J_{12} = 10$ Hz; weak coupling is assumed between the two spins. No weighting functions were used, and the spectrum is displayed in magnitude mode.

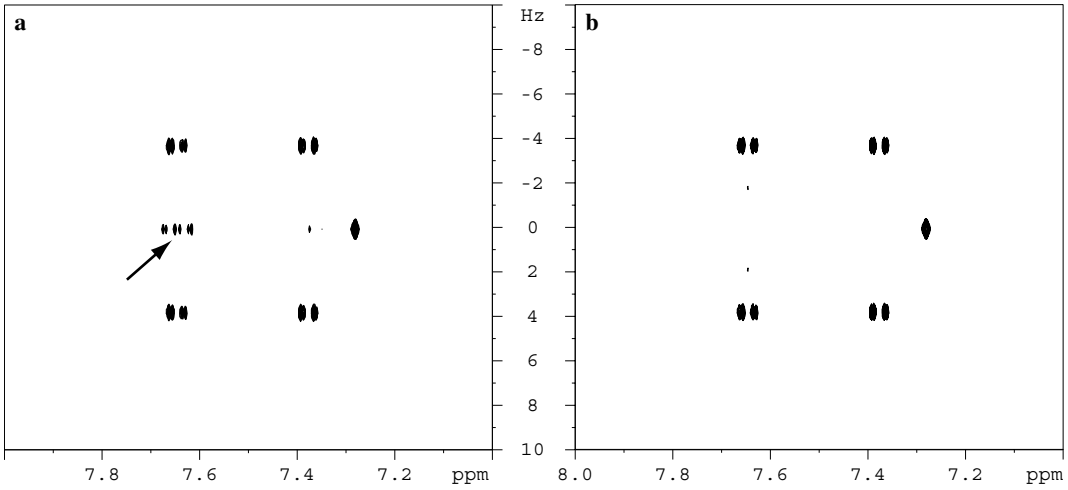

Fig. 5. J-resolved spectra of aspirin with selective refocusing of H4 (7.62 ppm) and H5 (7.36 ppm) protons. (a) single spin-echo; (b) double spin-echo. Eight scans were collected for each of the 64 t_1 increments and the standard processing (see Section 3) was complemented with symmetrization. Both spectra, acquired with the same experimental setup, are cut above the same threshold level. The spectrum obtained from a single spin-echo displays an artifactual pattern (marked with an arrow) that is virtually absent in the double spin-echo analogue. The peak at 7.28 ppm is from residual $CHCl_3$.

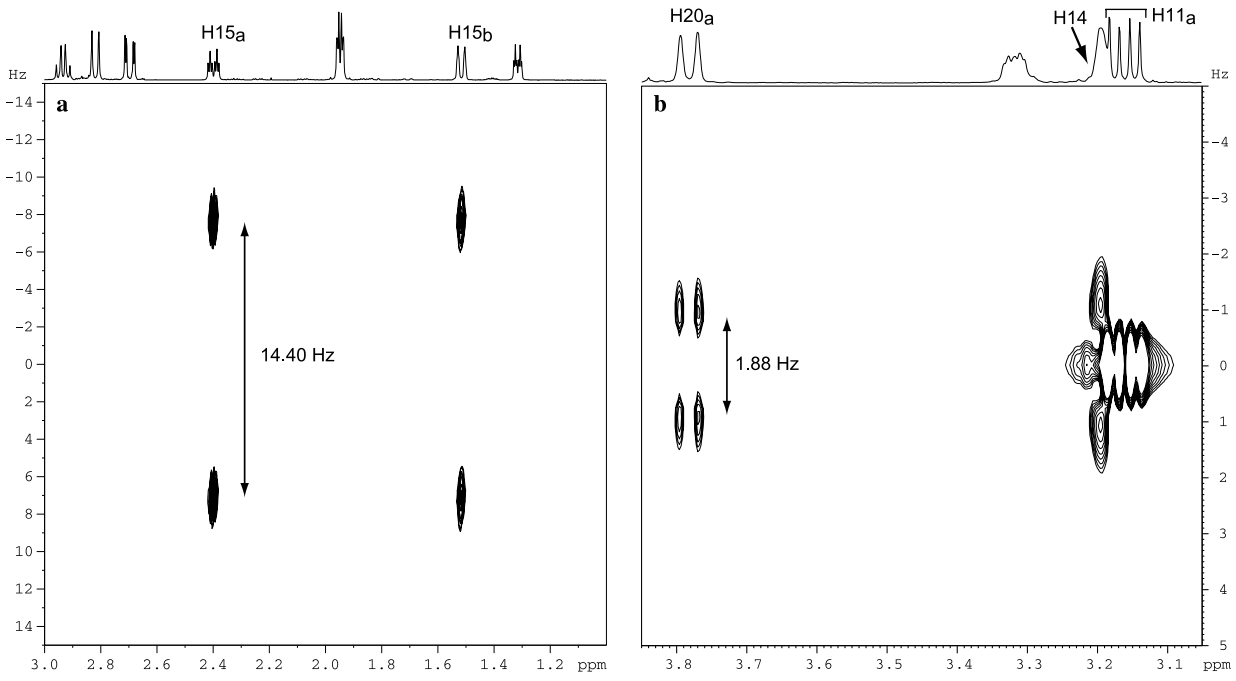

Fig. 6. Selective *J*-resolved spectra of strychnine. (a) Non-symmetrized spectrum obtained from selective refocusing of the geminal H15a and H15b protons. (b) Symmetrized spectrum obtained from selective refocusing of protons H20a and H14 + (partially) H11a. Eight scans were collected for each of the 32 t_1 increments. Apodization with non-shifted sinebell functions in both dimensions was employed prior to Fourier transformation.

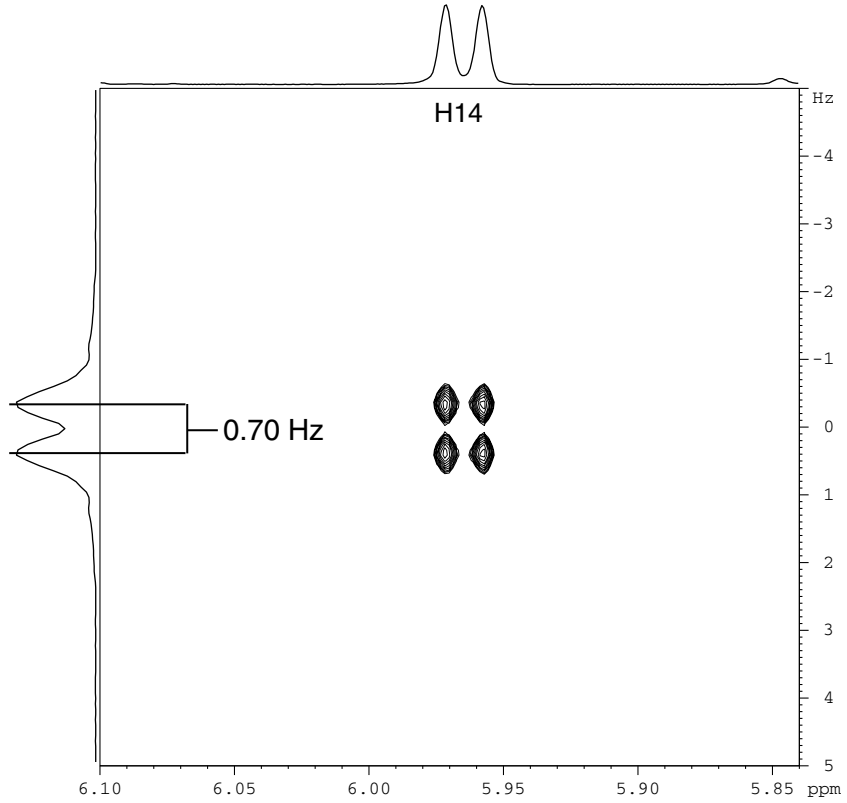

Fig. 7. Expanded region of the selective *J*-resolved spectrum of retinal obtained by selective refocusing of protons H14 and H11 (not shown). The top trace is the full ^{1}H spectrum, while the left trace is a projection of the signals visible in the *J*-resolved spectrum. Eight scans were collected for each of the 64 t_1 increments; zero-filling up to a total of 128 data points results in a digital resolution of 0.12 Hz. The standard processing (see Section 3) was complemented with symmetrization.

the assumption of weak coupling [15], and folding-back in the *J*-dimension occurs whenever the spectral window is narrowed below this range. Therefore, rather than adding further complication, folding-back itself tends to break the symmetry of strong coupling artifacts in such way that clean *J*-resolved spectra can be obtained by simple symmetrization. Much more often, the major source of unwanted signals in the *J*-dimension stems from miscalibration of the soft pulses. As an example, Fig. 5 compares the quality of two biselective *J*-resolved spectra obtained from single and double spin-echo pulse sequences, without precalibration of the soft pulses. For a spectrometer operating at 300 MHz, the aromatic ring protons of aspirin (**1**) are coupled strongly enough to observe artifactual patterns in a full *J*-resolved spectrum. Nonetheless, when the soft pulses are set to refocus protons H4 and H5, the tilted and symmetrized spectrum obtained from the single spin-echo pulse scheme displays just an additional zero-frequency signal in the indirect dimension due to imperfect refocusing of H5 resonance (Fig. 5a). No residual strong coupling artifacts are observed and, as expected, the much smaller zero-frequency signal falls below the adopted cutoff threshold in the tilted and symmetrized spectrum obtained from the double spin-echo pulse scheme (Fig. 5b).

4.2. Strychnine

Two representative spectra of the strychnine sample are reported in Fig. 6: panel (a) displays a biselective *J*-resolved spectrum obtained by refocusing H15a and H15b, while spectrum (b) was obtained by refocusing H20a and H14. In this second case, the soft pulse could not avoid a partial refocusing of H11a: yet this signal does not evolve in the indirect dimension because H11a does not couple significantly with H20a or H14. As a result, even though the signals from H14 and H11a are partially overlapped, the active coupling is again evident, even if its value is more clearly determined from the splitting of H20a. For this spin pair we have found a coupling constant of 1.88 Hz, to be compared with 1.55 Hz of Ref. [16]. Moreover, we were also able to directly measure a coupling constant of 3.12 Hz between H22 and H14, a value so far estimated to be 2.82 Hz only by modified *J*-doubling methods [17].

4.3. Retinal

The conjugated polyene backbone of all *trans*-retinal (**3**) provides a rigid and planar conformation where small H–H long-range couplings are likely to occur. Thus, we adopted this molecule as a model to explore the resolution limit of the biselective *J*-resolved method, and we focused on measuring the value of $^5J_{H11,H14}$ which has been previously reported (by means of *J*-resolved spectroscopy) to lie in the range 0.6–1.0 Hz [18]. In order to achieve the maximum possible resolution in the indirect dimension, a spectral window of 20 Hz was set and 64 t_1 increments were collected (a narrower spectral window would require much too long t_1 increments to observe any residual echo signal).

As shown in Fig. 7, we found a $^5J_{H11,H14} = 0.70$ Hz for the H11–H14 spin pair. The large passive coupling (8.11 Hz) which appears in the direct dimension mainly originates from $^3J_{H14,H15}$.

4.4. Determination of H^{α} couplings in a tripeptide

In looking for a possible application of the biselective *J*-resolved pulse scheme, we have chosen to determine the coupling constants for Met H^{α} in the chemoattractant tripeptide f-Met-Leu-Phe-OMe [19]. When this peptide is dissolved in acetonitrile and a proton spectrum is acquired at 300 MHz, the HN region exhibits overlapped signals that preclude a direct estimate of $J_{HNH\alpha}$ coupling constants. Of course, one may well resort to COSY or E.COSY techniques to circumvent this problem: nonetheless, while the $J_{HNH\alpha}$ coupling constants become accessible, Met $H^{\beta2/\beta3}$ signals still exhibit wide multiplet patterns that give rise to rather weak and poorly resolved cross-peaks. As an alternative, deconvolution of H^{α} multiplets (e.g., by modified *J*-doubling methods [17]) would only provide three *J* values with no specific assignments.

In such context, a *J*-resolved spectrum obtained from selective refocusing of Met H^{α} and Met $H^{\beta2/\beta3}$ offers a

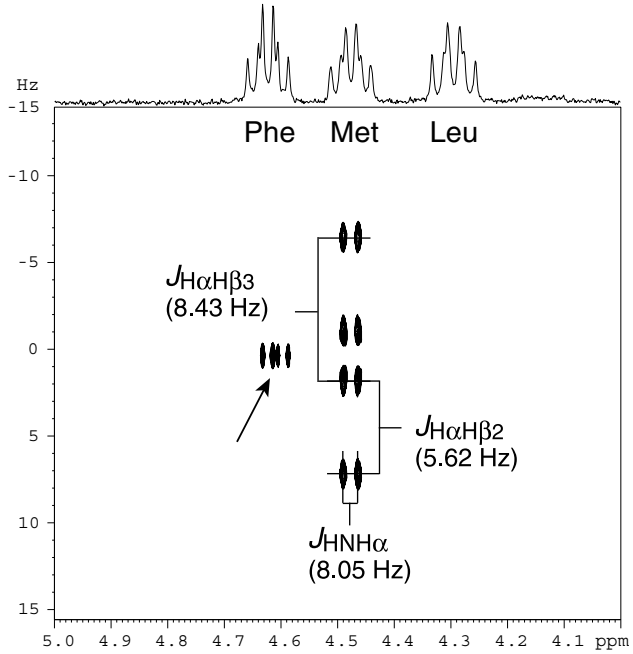

Fig. 8. H^{α} region of the selective *J*-resolved spectrum of f-Met-Leu-Phe-OMe (10 mM in CD_3CN). Resonances of Met H^{α} and Met $H^{\beta2/\beta3}$ were refocused by a 18 ms Gaussian and a 33 ms REBURP pulse, respectively (the arrow marks a small residual signal from the Phe H^{α} multiplet which is also partly refocused). Since a semi-selective pulse was employed on Met $H^{\beta2/\beta3}$, *J*-couplings of these protons to H^{α} are arbitrarily labelled and could be interchanged. Eight scans were collected for each of the 32 t_1 increments; the standard processing (see Section 3) was complemented with symmetrization. Top trace shows a full ^1H spectrum.

straightforward solution to the problem, since the active couplings $J_{H\alpha H\beta 2}$ and $J_{H\alpha H\beta 3}$ are resolved in the indirect dimension while the passive coupling $J_{HNH\alpha}$ appears in the direct dimension (Fig. 8).

5. Conclusions

Various techniques may lead to precise and accurate measurements of homonuclear coupling constants. Among these, *J*-resolved spectroscopy has recently benefited from a revamp aiming at the suppression of the so-called "strong coupling artifacts". Following these improvements, we have devised a biselective *J*-resolved pulse sequence that allows for unambiguous measurements of coupling constants between single spin pairs. Being based on the DPFGSE approach, this pulse sequence does not produce those phase defects typically observed when soft pulses are employed, and is quite tolerant to pulse miscalibration as well. The proposed examples show potential applications of this method in organic chemistry, ranging from complex natural substances to molecules of biological interest.

Acknowledgments

This work was financially supported by the University of Padova (Progetto di Ricerca di Ateneo CPDA045589). We are grateful to Dr. D. Frezzato and Professor S. Mammi for helpful comments on the manuscript. The tripeptide was kindly provided by Professor C. Toniolo.

References

[1] S. Simova, H. Sengstschmid, R. Freeman, Proton chemical-shift spectra, J. Magn. Reson. 124 (1997) 104–121.
[2] M. Kaupp, M. Bühl, V.G. Malkin (Eds.), Calculation of NMR and EPR Parameters, Wiley-VCH, Weinheim, 2004.
[3] A. Bagno, F. Rastrelli, G. Saielli, Predicting ^{13}C NMR spectra by DFT calculations, J. Phys. Chem. A 107 (2003) 9964–9973.
[4] A. Bagno, G. Saielli, F. Rastrelli, Toward the complete prediction of the ^{1}H and ^{13}C NMR spectra of complex organic molecules by DFT methods. Application to natural substances, Chem. Eur. J. 12 (2006), doi:10.1002/chem.200501583.
[5] T. Fäcke, S. Berger, SERF, a new method for H,H spin-coupling measurement in organic chemistry, J. Magn. Reson. A 113 (1995) 114–116.
[6] T.-L. Hwang, A.J. Shaka, Water suppression that works. Excitation sculpting using arbitray waveforms and pulsed field gradients, J. Magn. Reson. A 112 (1995) 275–279.
[7] S. Bourg, J.M. Nuzillard, In-phase double selective excitation of coupled spin systems using excitation sculpting, J. Magn. Reson. 133 (1998) 173–176.
[8] R.R. Ernst, G. Bodenhausen, A. Wokaun, Principles of Nuclear Magnetic Resonance in One and Two Dimensions, Clarendon Press, Oxford, 1987.
[9] T. Parella, F. Sanchez-Ferrando, A. Virgili, A simple approach for ultraclean multisite selective excitation using excitation sculpting, J. Magn. Reson. 135 (1998) 50–53.
[10] G.S. Armstrong, J. Chen, K.E. Cano, A.J. Shaka, V.A. Mandelshtam, Regularized resolvent transform for direct calculation of 45° projections of 2D *J* spectra, J. Magn. Reson. 164 (2003) 136–144, and references therein.
[11] P. Mutzenhardt, F. Guenneau, D. Canet, A procedure for obtaining pure absorption 2D *J*-spectra: application to quantitative fully *J*-decoupled homonuclear NMR spectra, J. Magn. Reson. 141 (1999) 312–321.
[12] A. Jerschow, Unwanted signal leakage in excitation sculpting with single axis gradients, J. Magn. Reson. 137 (1999) 206–214.
[13] A. Bax, R. Freeman, G.A. Morris, A simple method for suppressing dispersion-mode contributions in NMR spectra: the "pseudo-echo", J. Magn. Reson. 43 (1981) 333–338.
[14] M.J. Thrippleton, R.A.E. Edden, J. Keeler, Suppression of strong coupling artefacts in *J*-spectra, J. Magn. Reson. 174 (2005) 97–109.
[15] G. Wider, R. Baumann, K. Nagayama, R.R. Ernst, K. Wüthrich, Strong spin-spin coupling in the two-dimensional *J*-resolved 360-MHz ^{1}H NMR spectra of the common amino acids, J. Magn. Reson. 42 (1981) 73–87.
[16] X. Miao, R. Freeman, Spin-echo modulation experiments with soft gaussian pulses, J. Magn. Reson. A 119 (1996) 90–100.
[17] J.C. Cobas, V. Constantino-Castillo, M. Martín-Pastor, F. del Río-Portilla, A two-stage approach to automatic determination of ^{1}H NMR coupling constants, Magn. Reson. Chem. 43 (2005) 843–848.
[18] J. Wernly, J. Lauterwein, Two-dimensional NMR studies of polyene systems. I. All-trans-retinal, Helv. Chim. Acta 66 (1983) 1576–1587.
[19] G. Cavicchioni, S. Spisani, The role of for-Met-Leu-Phe amide bonds on chemotactic receptor–ligand cross-linking, Curr. Topics Peptide Protein Res. 2 (1997) 33–39.